Received: 22 July 2020 | Accepted: 30 September 2020

DOI: 10.1002/vzj2.20084

Vadose Zone Journal

TECHNICAL NOTE

Quantification of hydraulic redistribution in maize roots using neutron radiography

Faisal Hayat[1] | **Mohsen Zarebanadkouki**[1] | **Mutez Ali Ahmed**[1] | **Thomas Buecherl**[2] | **Andrea Carminati**[1]

[1] Chair of Soil Physics, Univ. of Bayreuth, Bayreuth, 95444, Germany

[2] Radiochemie München, Technische Univ. München, Garching 85748, Germany

Correspondence
Faisal Hayat, Chair of Soil Physics, Univ. of Bayreuth, Bayreuth, 95444, Germany.
Email: Faisal.Hayat@uni-bayreuth.de

Assigned to Associate Editor Quirijn de Jong van Lier.

Abstract

Plants redistribute water from wet to dry soil layers through their roots, in the process called hydraulic redistribution. Although the relevance and occurrence of this process are well accepted, resolving the spatial distribution of hydraulic redistribution remains challenging. Here, we show how to use neutron radiography to quantify the rate of water efflux from the roots to the soil. Maize (*Zea mays* L.) plants were grown in a sandy substrate 40 cm deep. Deuterated water (D_2O) was injected in the bottom wet compartment, and its transport through the roots to the top dry soil was imaged using neutron radiography. A diffusion–convection model was used to simulate the transport of D_2O in soil and root and inversely estimate the convective fluxes. Overnight, D_2O appeared in nodal and lateral roots in the top compartment. By inverse modeling, we estimated an efflux from lateral roots into the dry soil equal to $j_r = 2.35 \times 10^{-7}$ cm^{-1}. A significant fraction of the redistributed water flew toward the tips of nodal roots (3.85×10^{-8} cm^3 s^{-1} per root) to sustain their growth. The efflux from nodal roots depended on the roots' length and growth rate. In summary, neutron imaging was successfully used to quantify hydraulic redistribution. A numerical model was needed to differentiate the effects of diffusion and convection. The highly resolved images showed the spatial heterogeneity of hydraulic redistribution.

1 | INTRODUCTION

Water is heterogeneously distributed in soils, and understanding how root water uptake and root growth respond to such heterogeneity is crucial to predict plant response to drought. Root water uptake from deep wet soil layers helps plants to tolerate drought periods (Sharp & Davies, 1985; Zegada-Lizarazu & Iijima, 2004). Besides sustaining the transpiration demand of plants, a fraction of the water extracted from the subsoil is redistributed within the root system to dry soil layers due to gradients in water potential in the process called hydraulic redistribution (HR; Burgess, Adams, Turner, & Ong, 1998; Caldwell & Richards, 1989; Richards & Caldwell, 1987). Hydraulic redistribution is also referred to as hydraulic lift when water moves from deep wet soil to top dry soil layers (Brooks, Meinzer, Coulombe, & Gregg, 2002; Smart, Carlisle, Goebel, & Núñez, 2005). Redistributed water can replenish up to 35% of the total daily used water from the upper 2 m of soil layers under drought conditions (Brooks et al., 2002). The redistributed water sustains root growth or life span of fine roots (Bauerle, Richards, Smart, & Eissenstat,

Abbreviations: D_2O, deuterated water; HR, hydraulic redistribution; LED, light-emitting diode; SWC, soil water content.

2008) and increases nutrient availability in drier soil (Caldwell, Dawson, & Richards, 1998; Snyder, James, Richards, & Donovan, 2008; Wang, Tang, Guppy, & Sale, 2009).

Although the occurrence, relevance, and amount of HR are well accepted and documented, resolving the spatial distribution of HR along the root system and into the soil remains challenging. Neutron radiography, thanks to its high sensitivity to water and thus to roots, is an imaging method with great potential to quantitatively estimate root distribution and water flow in soil and roots (Moradi et al., 2011; Oswald et al., 2008). Warren, Bilheux, Kang, et al. (2013) used neutron radiography and deuterated water (D_2O) to trace HR in seedlings of *Zea mays* L. and *Panicum virgatum* L. The authors showed a high sensitivity of neutron radiography to small changes in D_2O concentrations, which enables them to visualize the translocation of D_2O through the roots of young plants.

Interpretation of time-series radiographs of D_2O is challenging (Carminati & Zarebanadkouki, 2013; Warren, Bilheux, Cheng, & Perfect, 2013), and several possible artifacts should be considered. The neutron attenuation coefficient of D_2O is much lower than that of H_2O. When D_2O replaces H_2O in a given root or soil region, the attenuation coefficient of that region largely drops, making the redistribution of D_2O visible over time. However, neutron attenuation does not depend only on the fraction of D_2O and H_2O, but also on the total content of liquid (the sum of D_2O and H_2O). This value changes in soils due to water uptake and HR and small increases (or decreases) in liquid content can cause significant underestimation (or overestimation) of the concentration of D_2O (Carminati & Zarebanadkouki, 2013). This problem is more critical for soils (whose moisture content easily varies from 0 to 0.4) than for roots. However, root shrinkage might similarly affect the interpretation of the neutron signal. An additional complexity is that the transport of D_2O in soils and plants depends on both diffusion and convection. It means that an increase (or decrease) of D_2O in roots and soil does not necessarily indicate a net flow into (or from) roots, but it might be caused by diffusion driven by gradients in D_2O concentration. Zarebanadkouki, Kroener, Kaestner, and Carminati (2014) conducted a series of D_2O tracing experiments during the day and nighttime and developed a numerical model simulating diffusion and convection of D_2O in soil and roots. The authors proved that the diffusion of D_2O from the root surface to its xylem is as significant as the convective fluxes, also during the daytime, and it should be properly modeled to quantify the local fluxes of water. The method was used for quantifying root water uptake in homogeneous soil moisture conditions (Ahmed, Zarebanadkouki, Kaestner, & Carminati, 2016; Ahmed et al., 2018), but it has not yet been tested to quantify the efflux of water from the roots during nighttime.

The objective of this technical note was to test whether the combination of neutron radiography, D_2O injection, and a diffusion–convection model allows quantification of HR and hydraulic lift. To test the feasibility of the method, we grew maize (*Z. mays*) plants in a sandy substrate that was partitioned into two horizontal compartments hydraulically separated by a 1-cm layer of coarse sand acting as a capillary barrier. When plants were well established, we let the upper compartment dry while we kept the lower compartment wet. Then D_2O was injected at the lower wet compartment, and its transport within the root system was monitored for a period of ~15 h (a daytime cycle followed by a nighttime cycle) using a time series neutron radiography. We also made two additional tests: (a) we injected H_2O instead of D_2O to monitor possible root shrinkage and swelling; and (b) we injected D_2O in a sample whose top and bottom compartments were both kept wet, to test the effect of diffusion on D_2O dynamics in the top compartment.

Core Ideas

- Measuring the spatial distribution of HR along the root system remains challenging.
- Neutron radiography was used to trace the transport of D_2O from wet to dry soil layers.
- Radial fluxes were estimated using diffusion–convection model of D_2O transport in soil and root.
- Water was redistributed from wet to dry soil layers through fine lateral roots.
- A fraction of HR water was used to sustain the growth of young nodal roots.

2 | MATERIALS AND METHODS

2.1 | Soil and plant preparation

Three maize plants were grown in aluminum containers (40 cm high, 40 cm wide, and 1 cm thick). The containers were filled with a mixture of silt and sand (1:1 ratio) with particle size <1 mm and a bulk density of 1.4 g cm^{-3}. A 1-cm layer of fine gravels (particle size of 2–2.5 mm) was placed at a depth of 20 cm to hydraulically disconnect the top and bottom soil compartments without hindering the root growth (similar to Ahmed et al. , 2016; Zarebanadkouki et al., 2012).

Maize seeds were germinated for 48 h and then planted in the containers (one seed per container). The soil surface was covered with fine gravels (particle size of 2–2.5 mm) to minimize evaporation. Plants were grown in a climate room with a photoperiod of 14 h (from 7:00 a.m. to 9:00 p.m.), day/night temperature of 24/19 ˚C, relative humidity of 60%, and light intensity of 750 µmol m^2 s^{-1}. Plants were irrigated every third day during the first 3 wk, allowing roots to grow uniformly

in both compartments. Afterwards, the soil water contents (SWCs) were adjusted in the top and bottom compartments to the following scenarios. First, in two plants, the top soil compartment was kept dry (SWC ≤0.06, corresponding to a matric potential <−1,000 hPa, as estimated according to the water retention measured in Hayat et al., 2020) and the bottom compartment was kept wet (SWC ≈ 0.22, corresponding to a water matric potential of approximately −80 hPa); we refer to this scenario as dry–wet. Second, in one plant, both compartments were kept wet (SWC ≈ 0.22); we refer to this scenario as wet–wet. Prior to neutron radiography experiments, a light-emitting diode (LED) lamp (GC 9, Greenception, with specifications of photon flux intensity at height of 30 cm above plant ≈ 1.800 µmol m^2 s^{-1} and maximum spectrum wavelength = 700 nm) was installed above the plants. The average transpiration at daytime of dry–wet and wet–wet samples was 4.66 ± 0.26 and 4.87 g h^{-1}, respectively. The neutron radiography measurements started when plants were 40 d old.

2.2 | Neutron radiography

Neutron radiography is a noninvasive imaging technique that allows for imaging water and root distribution in the soil (Carminati et al., 2010; Tumlinson, Liu, Silk, & Hopmans, 2008; Zarebanadkouki, Kim, & Carminati, 2013). The transmitted neutrons beam carries the information of the sample composition and thickness. The Beer–Lambert law describes the attenuation of the neutron beam (Kasperl & Vontobel, 2005) through the sample by

$$\frac{I}{I_0} = \exp\left[-\sum_{i=1}^{i=n}\left(\mu_i d_i\right)\right] \quad (1)$$

where I is the detected neutron intensity (cm^{-2} s^{-1}), I_0 is the incident neutron intensity (cm^{-2} s^{-1}), μ_i is the neutron attenuation coefficient (cm^{-1}), and d_i is the thickness (cm) of the material i. The material composing our samples were aluminum, dry soil, root (here intended as dry mass), water (H_2O), and deuterated water (D_2O). The attenuation of dry soil and aluminum were derived from the radiograph of a container filled with dry soil. The attenuation coefficients of H_2O and D_2O were experimentally estimated from the radiograph of control samples with a known thickness of normal and deuterated water.

The neutron radiography experiments were carried out at the NECTAR (neutron computed tomography and radiography) facility (Bücherl & Söllradl, 2015) at the Heinz Maier-Leibnitz center, Technical University Munich (TUM), using its new option of thermal neutron radiography (Mühlbauer et al., 2018).

The thermal neutron spectrum is provided at the measurement position through a flight tube of 4 m in length with an entrance aperture of 25 mm in diameter. This resulted in a calculated length/diameter ratio of 240 and a measured integral neutron intensity of 7.9 × 10^6 cm^{-2} s^{-1} at the sample position. The detector system consists of a ^{6}LiF/ZnS scintillator screen of 100-µm thickness, which converts the neutrons into light, which is mirrored on a Andor iKon-L-BV charge-coupled device (CCD) camera (Model DZ936N BV) with 2,048 × 2,048 px and a pixel size of 13.5 ×13.5 µm. The CCD camera was operated at a temperature of −97 ˚C, thus having a dark current of <0.0001 electrons px^{-1} s^{-1}.

The samples were placed as close as possible to the scintillator screen of the detector system (i.e., at a distance of ~3 cm). This setup corresponds to a quasiparallel neutron beam geometry.

A complete set of data for one radiograph consisted of dark current images (i.e., images with the camera shutter and the neutron beam closed), flat field images (i.e., images without sample), and images with a sample. All images were recorded for 20 s each. From a series of dark images and flat field images, the mean dark image $I_{DC}(x, y)$ and the flat field image $I_{FF}(x, y)$ were calculated, respectively. As the sample sizes were larger than the beam area, succeeding measurements at two vertical and two horizontal positions each could be performed to scan the complete sample on a two-by-two grid with overlapping margins.

An identical LED lamp, used prior to neutron radiography, was installed above the plants during the day measurements.

2.3 | D_2O tracing experiment

Deuterated water (D_2O) was used to trace the flow of water in soil and roots. Due to its lower neutron attenuation coefficient compared with H_2O, D_2O is easily distinguishable in neutron radiographs. We injected 30 ml of D_2O (purity of 99.97%) at two selected locations in the bottom wet compartment (15 ml at each location) using fine syringes (Figure 1). The spatiotemporal distribution of D_2O in each compartment and its transport along the roots were monitored by time-series neutron radiography with a temporal resolution of one frame every 20 s. The D_2O tracing measurements started during the daytime (between 4:30 and 6:00 p.m.) and continued till the next morning (around 8:00 a.m.). The light was turned off at 7:00 p.m. and turned on again at 7:00 a.m. The samples were not moved throughout the time series to avoid artifacts due to imprecise referencing. The reconstructed image of one entire sample before injection of D_2O is shown in Figure 1. The image was obtained by overlapping four radiographs. The gray values show the water content in the sample (i.e., the darker the image, the higher the SWC). As roots have high water content, they appear dark. The roots in which D_2O transport is quantified are shown in colors. Here, three different root types are selected: seminal roots reaching the

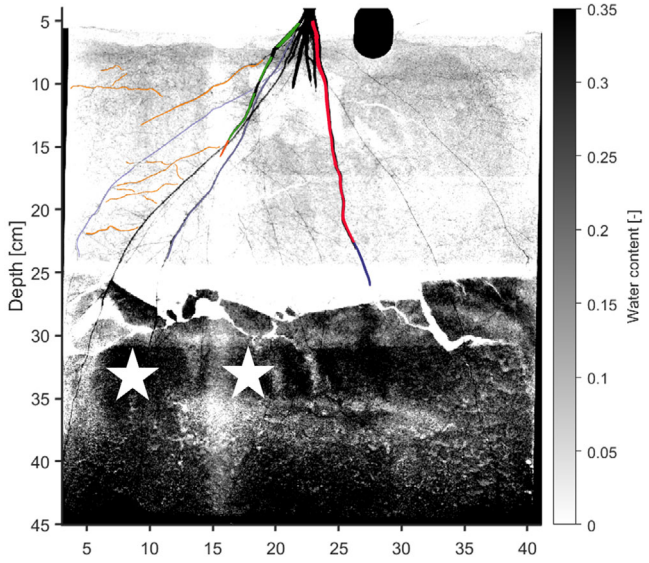

FIGURE 1 Reconstructed image of the one sample (dry–wet) before the injection of deuterated water (D_2O). The stars indicate the locations where D_2O was injected (in the bottom compartment). The image was obtained by overlapping four radiographs. The gray values represent water content (the darker the image, the higher the soil water content). The segmented roots in which we quantified the D_2O concentration are shown in light purple, orange, and red + green colors and are categorized as seminal roots, laterals, and nodal (long + short), respectively

bottom compartment and immersed in D_2O after D_2O injection, lateral roots, and nodal roots with their tips in the top compartment.

2.4 | Control experiments

To ensure that the D_2O measurements were correctly interpreted (see Section 4), in one of the samples of the dry-wet scenario, we first injected 30 ml of H_2O in the bottom wet compartment and monitor water redistribution within the root system overnight. The D_2O was injected 24 h later.

2.5 | Image analysis

The obtained neutron radiographs were normalized for the flat field (radiograph without sample) and dark current (signals recorded by the camera in the absence of a beam) as

$$I_{\text{norm}}(x,y,t) = \frac{I(x,y,t) - I_{\text{DC}}(x,y)}{I_{\text{FF}}(x,y) - I_{\text{DC}}(x,y)} \times \frac{D_0}{D(t)} \tag{2}$$

where x and y refer to the spatial coordinates of pixels in the x and y direction, t refers to the time after D_2O injection, $I_{\text{norm}}(x, y, t)$ is the normalized image, $I(x, y, t)$ is the recorded image at time t, $I_{\text{DC}}(x, y)$ is the dark current image, $I_{\text{FF}}(x, y)$ is the flat field image, and D_0 and $D(t)$ are scalar values proportional to the neutron attenuation at time zero and any given time t in a blank area of radiographs, respectively. By combining the Beer–Lambert law for these samples,

$$\begin{aligned} &-\log\left[I_{\text{norm}}(x,y,t)/I_{\text{dry}}(x,y)\right] \\ &\quad = \mu_{\text{H2O}}\, d_{\text{H2O}}(x,y,t) + \mu_{\text{D2O}}\, d_{\text{D2O}}(x,y,t) \end{aligned} \tag{3}$$

where $I_{\text{dry}}(x, y)$ is the radiography of the dry sample, μ_{H2O} (cm^{-1}) and d_{H2O} (cm) are the attenuation coefficient and thickness of normal water (H_2O), and μ_{D2O} (cm^{-1}) and d_{D2O} (cm) are the attenuation coefficient and thickness of heavy water (D_2O). The measured attenuation coefficients for normal water (μ_{H2O}) and deuterated water (μ_{D2O}) were 1.04 and 0.335 cm^{-1}, respectively. The sharp difference in water contents between roots and the surrounding soil allowed us to segment roots. We segmented roots using Matlab 2019b (MathWorks). The length and diameter of segmented roots were calculated using the Euclidean distance mapping functions in Matlab 2019b.

The concentration of D_2O within the roots was calculated according to the protocol presented in Zarebanadkouki et al. (2012). We define $\mu_{\text{root}}(t)$ (cm cm^{-1}) as the neutron attenuation in the pixel containing roots as

$$\mu_{\text{root}}(t) = -\log\left[\frac{I_{\text{norm}}(x,y,t)}{I_{\text{dry}}(x,y)}\right]\frac{1}{d_{\text{root}}} \tag{4}$$

where d_{root} is the root thickness (cm). We assumed that the volumetric liquid content of the root tissue did not change after immersion in D_2O. It follows that

$$d_{\text{root}}^{\text{H2O}}(t=0) = d_{\text{root}}^{\text{D2O}}(t) + d_{\text{root}}^{\text{H2O}}(t) \tag{5}$$

Then, the pixel-wise concentration of D_2O in the pixel containing root can be calculated as

$$C_{\text{D2O, root}} = \frac{d_{\text{root}}^{\text{D2O}}}{d_{\text{root}}^{\text{liq}}} \tag{6}$$

where

$$d_{\text{root}}^{\text{D2O}} = \frac{\left[\mu_{\text{root}}(t) - \mu_{\text{root}}(t=0)\right] d_{root}}{\mu_{\text{D2O}} - \mu_{\text{H2O}}} \tag{7}$$

The total liquid thickness in the root ($d_{\text{root}}^{\text{liq}}$) was calculated as H_2O thickness in the first radiograph before D_2O was injected [i.e.,$d_{\text{root}}^{\text{liq}} = d_{\text{root}}^{\text{H2O}}(t=0)$]. Here, we assumed that the change in pixel-wise water content of the soil in the upper compartment is negligible. The concentration of D_2O in the root was averaged along the root segment.

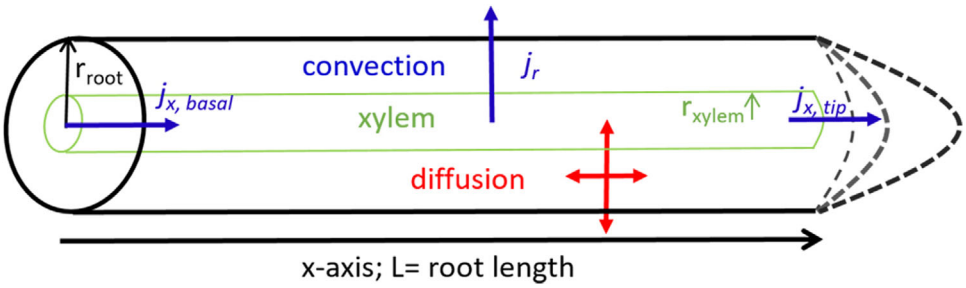

FIGURE 2 Illustration of the deuterated water (D_2O) transport model into the root. Here, red and blue arrows show diffusive and convective fluxes, respectively. Radial water fluxes j_r can be directed toward the root surface (water uptake) or toward the soil (hydraulic lift). Axial fluxes could be toward the root tip (to sustain growth and hydraulic lift) or toward the basal part (to sustain transpiration)

We calculated the growth rate of roots assuming that water constitutes the major fraction of the root tissue:

$$\Delta V_{\text{root}}^{\text{H2O}} = \sum \left\{ \frac{\left[\mu_{\text{root}}(t) - \mu_{\text{root}}(t=0)\right] d_{\text{root}}}{\mu_{\text{H2O}}} \right\} \times \text{Res}^2 \tag{8}$$

where the right-hand side of Equation 8 refers to the summation of neutron attenuation in both x and y coordinates of pixels containing root tissue, $\mu_{\text{root}}(t)$ refers to the average neutron attenuation across the thickness of root tissue in the radiographs, and Res is the pixel size.

We calculated the concentration of D_2O in three different root types in the top soil compartment as illustrated in Figure 1. The first were seminal and primary root segments that reached the bottom compartment where D_2O was injected. These roots took up D_2O from the soil and transported it axially upwards towards the shoot via transpiration stream; we refer to these roots as seminal roots. The second were lateral roots that were located in the top compartment and were not immersed in D_2O but received D_2O from the seminal roots; we refer to these roots as lateral roots. The third were nodal and crown roots located in the top compartment and that had not yet crossed the capillary barriers and reached the D_2O injected compartment; we refer to these roots as nodal roots. The second and third types of roots could only receive D_2O from the root–shoot conjunction.

2.6 | Model of D_2O transport into roots

To derive the fluxes of water from the temporal dynamics of D_2O concentration, we used a diffusion–convection model (Ahmed et al., 2016, 2018; Zarebanadkouki et al., 2014). The transport of D_2O in roots and soil depends on (a) diffusion due to gradients in the concentration of D_2O in soil and root and (b) convection due to water fluxes driven by transpiration and HR.

We simulated the D_2O transport in a single root, in which water flows axially along the xylem and radially across the cortex (Figure 2). The change in D_2O concentration in the root is described by

$$\theta \frac{\partial C}{\partial t} = \frac{\partial}{r\partial r}\left[rD\left(\frac{\partial C}{\partial r}\right)\right] - \frac{\partial}{r\partial r}\left(rj_r C\right) - \frac{\partial}{\partial x}\left(j_x C\right) \tag{9}$$

where $\theta(r, x)$ is the water content ($cm^3\ cm^{-3}$), $C(r, x, t)$ is the D_2O concentration in the root ($cm^3\ cm^{-3}$), t is the time (s), r is the radial coordinate (cm), x is the longitudinal coordinate (cm), $j_r(r)$ is the radial flux of water ($cm\ s^{-1}$), $j_x(r, x)$ is the axial flux of water ($cm\ s^{-1}$), and D is an effective diffusion coefficient of D_2O ($cm^2\ s^{-1}$). The axial flux of water within the root xylem is estimated by mass conservation equation, assuming that the axial transport of D_2O occurs only in the root xylem, as

$$\pi r^2 \frac{\partial j_x(x)}{\partial x} = -2\pi r j_r \tag{10}$$

where the j_x changes along x and j_r is assumed to be uniform along x. The water flux into the roots at the basal part is referred to as $j_{x,\text{basal}}$ and at the root tip is called $j_{x,\text{tip}}$ (Figure 2). The axial fluxes can be positive or negative and indicate HR and water uptake, respectively (x increases toward the root tip). A positive j_r indicates the efflux of water from the root to the soil and negative j_r indicates root water uptake.

2.7 | Model implementation

We modeled the transport of D_2O into roots in the top soil that had no direct access to D_2O from the soil (lateral and nodal roots, Figure 1). The D_2O transport was simulated in single roots (no branching) from their basal parts to the root tips. As roots grew during the measurements (16 h), root growth was included as convective flux toward the root tip (see below).

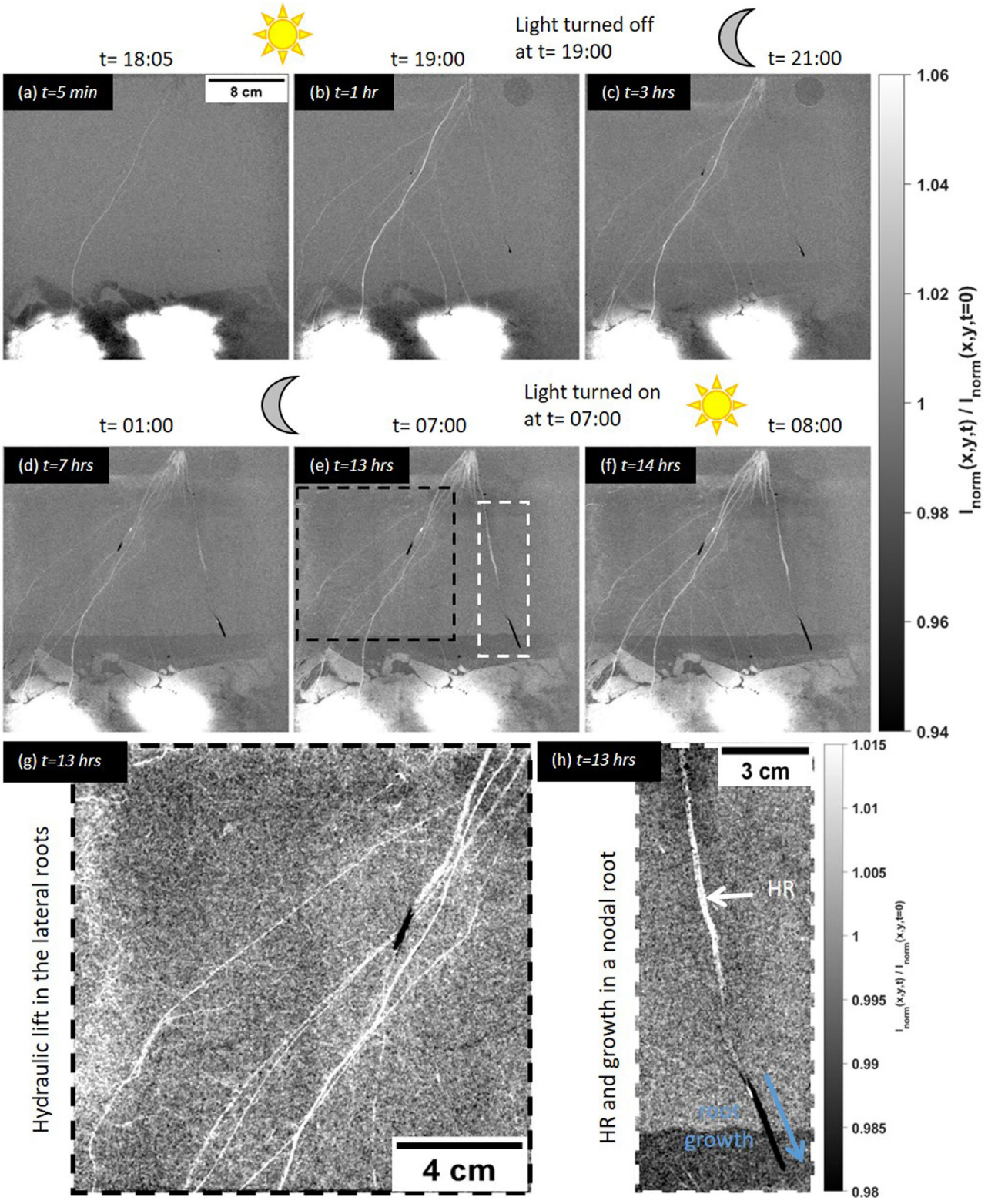

FIGURE 3 Neutron radiographs of deuterated water (D_2O) injection in a sample with dry top compartment and wet bottom compartment. The radiographs show the difference between the actual radiograph at time t and the one before D_2O injection. Panels a–f show the D_2O transport during day and its redistribution overnight. Panels g and h are zoom-in of the radiograph (e). Brighter colors indicate higher D_2O concentration, and dark colors indicate root growth. $I_{norm}(x,y,t)$ and $I_{norm}(x,y,t = 0)$ are the normalized radiographs at spatial coordinates in x and y direction at time t and at $t = 0$, respectively. HR denotes hydraulic redistribution

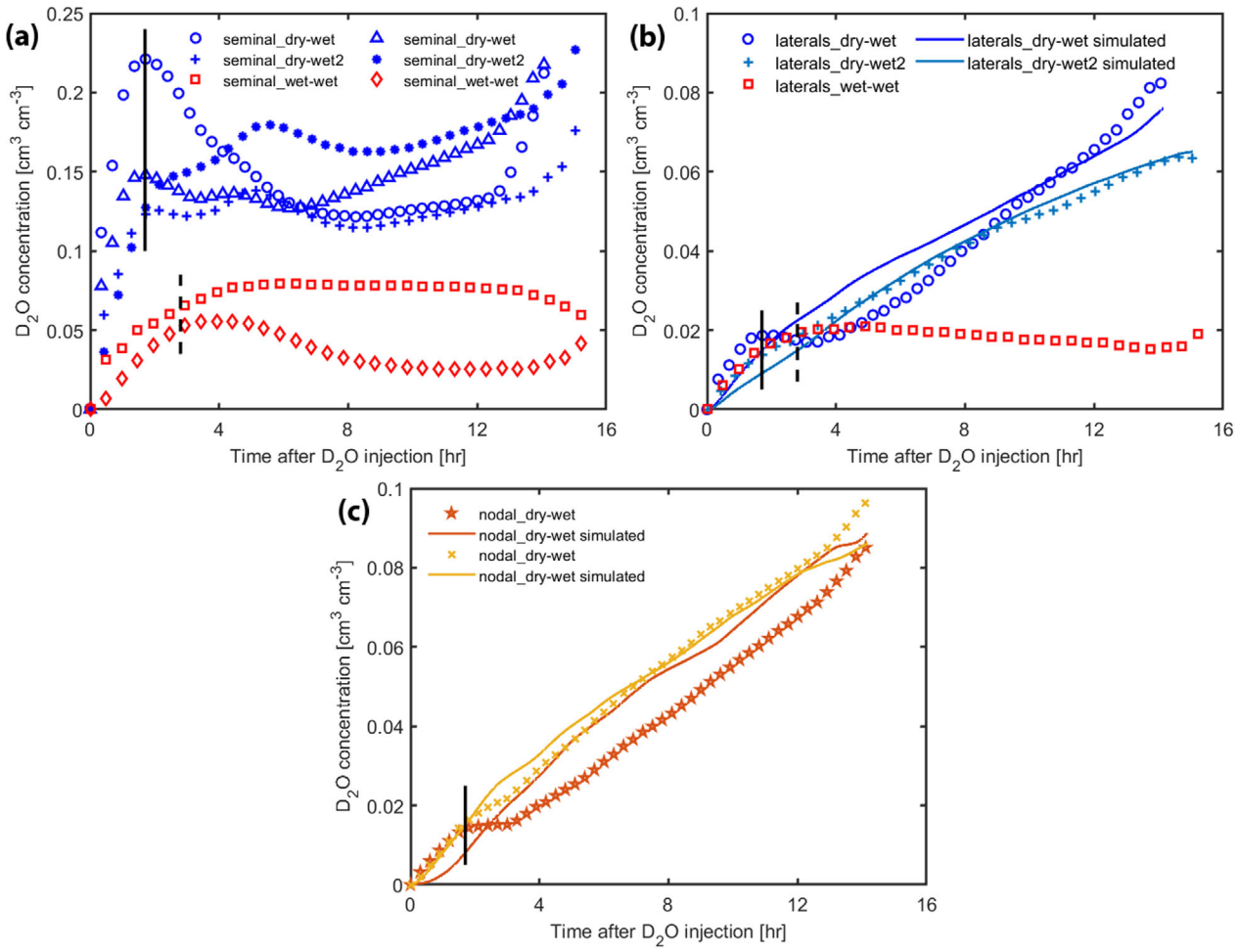

FIGURE 4 Average concentration of deuterated water (D_2O) in (a) seminal, (b) lateral, and (c) nodal roots in both dry–wet and wet–wet scenarios. The best fits of the model are shown for the dry–wet scenario (b and c). The vertical solid and dashed black lines show when the light was turned off in the two dry–wet and wet–wet samples, respectively. The R^2 values for the laterals of the two dry–wet samples are .89 and .98, respectively. The R^2 values for the nodal roots are .86 and .96

The diffusion–convection equation (Equation 9) was numerically solved in radially symmetric coordinates using a finite difference method. The flow domain from soil towards the root xylem and from the tip roots towards the basal parts were represented in a two-dimensional computational grid with 40 equally spaced grid elements along the root radius and 110 grid elements along the root length. The diffusion–convection equation was solved assuming the following initial and boundary conditions:

$$C(r, x, t = 0) = 0$$

$$\frac{\partial C(r = 0, x, t)}{\partial r} = 0$$

$$C\left(r \le r_{\text{xylem}}, x = x_{\text{basal}}, t\right) = C_0(t)$$

$$j_r\left(r = r_{\text{out}}\right) = \frac{r_{\text{root}}}{r_{\text{out}}} j_{\text{root}}$$

$$j_x\left(r \le r_{\text{xylem}}, x = x_{\text{tip}}, t\right) = j_{x,\text{tip}}(t)$$

$$j_x\left(r \le r_{\text{xylem}}, x = x_{\text{basal}}, t\right) = j_{x,\text{basal}}(t)$$

where $r = 0$ is the root center, r_{out} is the outer radius of soil (radius of the root, r_{root}, plus the thickness of soil used in our simulation), C_0 is the quantified D_2O concentration at the root surface in the soil during the measurements, j_{root} is the radial flux of water at the root surface, $x = x_{\text{tip}}$ refers to the position of the root tip, $j_{x,\text{tip}}$ is the axial flux of water at the root tip, x_{basal} refers to the position of the root at its basal part, at which the root segment was connected to the seminal roots (for the case of lateral roots) and the root-–shoot conjunction (for the case of crown roots), and $j_{x,\text{basal}}$ is the axial flux that the basal parts of each root segment. The diffusion coefficient of D_2O in the soil was taken from the value of diffusion coefficient D_2O in free water and scaled for the porosity and SWC, according to Millington and Quirk (1959). The

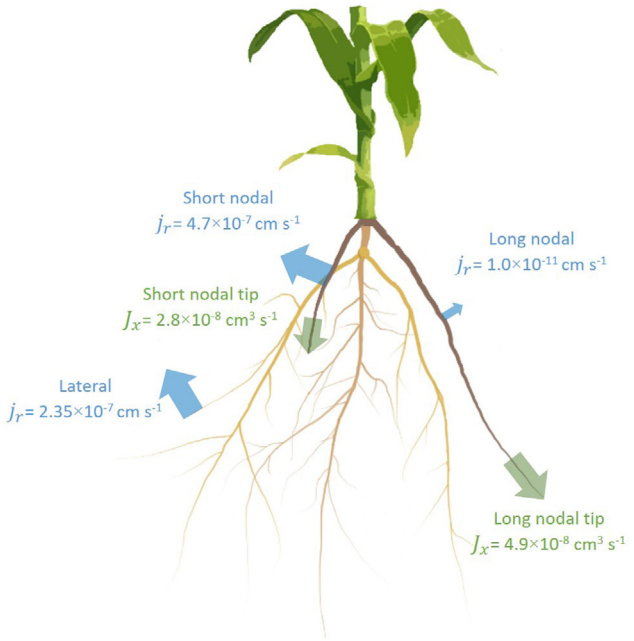

FIGURE 5 Summary of estimated fluxes along the measured root maize system. The fluxes of water from the root to the soil are shown in blue. The fluxes of water toward the root tip to sustain root growth are shown in green. j_r is the radial flux of water and J_x is the axial flow of water

values of diffusion coefficient across the root tissues were taken from Ahmed et al. (2016). The inverse problem was solved in Matlab (2019b) using the patternsearch solver from its optimization toolbox.

3 | RESULTS

Some selected neutron radiographs at different times after D_2O injection in one of the two dry–wet samples are presented in Figure 3 (same plant as shown in Figure 1). The radiographs show the difference between the actual radiograph and that before D_2O injection. The brighter is the color the higher is the D_2O concentration. Shortly after being injected, D_2O was taken up by seminal roots and was axially transported upwards towards the shoot following the transpiration stream (Figure 3a). During nighttime (from 7:00 p.m. to 7:00 a.m.), the lateral roots that were not in direct contact with D_2O in the injected compartment gradually turned bright. Similarly, the nodal roots that were not in direct contact with D_2O in the injected compartment also turned gradually bright. With time, the tip of nodal roots grew and appeared dark in the radiographs (Figure 3e). These observations (lateral roots turning bright over time) were consistent in the second sample (Supplemental Figure S1).

In the sample in which both top and bottom compartments were kept wet (Supplemental Figure S2), no increase of D_2O in lateral and nodal roots was detectable overnight. When only H_2O was injected, lateral roots did not change their attenuation coefficient, indicating that neither shrinking nor swelling were detectable. The latter experiment was done to exclude that the increasing root transparency (observed in the case of the dry–wet scenario) was caused by root shrinkage.

The average D_2O concentrations in roots located in the top compartment are shown in Figure 4. In seminal roots, the concentration of D_2O increased shortly after D_2O injection during daytime, and then it decreased and reached rather constant values during nighttime. The concentration increased again as transpiration restarted in the next morning. In the dry–wet scenario, D_2O concentration in lateral roots progressively increased during the nighttime. On the contrary, lateral roots in the wet–wet scenario showed a slight increase in the concentration of D_2O only in the first hour when the plant was still transpiring, whereas there was no increase overnight. Finally, we also plot the D_2O concentration in the nodal roots, which was similar to those of the laterals.

We used the diffusion–convection model (Equation 9) to simulate the measured D_2O concentration in laterals and nodal roots in the dry–wet scenarios. By inversely fitting the measured concentrations, we quantified the radial fluxes (j_r) of water during the night. The best fits are shown as solid lines in Figures 4b and 4c. The radial flux of water into or out of the root (j_r) was the only unknown parameter which was inversely adjusted. The best fits for the laterals in the two dry–wet samples were $j_r = 2.4 \times 10^{-7}$ and $j_r = 2.3 \times 10^{-7}$ cm s^{-1}, respectively. For the nodal roots, which grew overnight, the axial flux at the root tips was set to be equal to the root growth. The radial fluxes varied between the two nodal roots. In the longer nodal root, it was negligible ($j_r = 1 \times 10^{-11}$ cm s^{-1}) as compared with the laterals, indicating that water was mainly redistributed to the dry soil through the laterals. Note that such a low flux is probably below the detection limit. However, this nodal root tip received a significant flux of water to sustain its growth ($j_x = 1.94 \times 10^{-4}$ cm s^{-1}). For the shorter nodal (denoted by the dark yellow color in Figure 4c), the estimated radial flux was $j_r = 5 \times 10^{-7}$ cm s^{-1}, which is close to the value measured for laterals.

4 | DISCUSSION AND CONCLUSIONS

We successfully showed that neutron radiography allows visualization of HR. Using a diffusion–convection model, the water fluxes in different root types were estimated. We performed two measurements with heterogeneous SWCs (top soil compartment dry and bottom soil compartment wet; i.e., dry–wet) and one with homogeneous SWC (both soil compartments wet; i.e., wet–wet). Additionally, in one of the two dry–wet samples, we injected H_2O the day before injecting D_2O. The experiments with H_2O and the wet–wet scenario

were needed to test whether the decreasing neutron attenuation in the roots in the top compartment overnight was caused by root shrinkage or diffusion of D_2O along the xylem (note that diffusion does not require a mass flow). The two tests showed no detectable decrease in neutron attenuation in the upper roots, which confirms our interpretation that HR (a convective flux of water from the bottom to the top soil layer through the roots) was responsible for the detected signal in the dry–wet scenarios.

In the dry–wet scenario, lateral roots slowly turned more transparent during nighttime. This observation can be explained by two processes: (a) the roots located in the upper dry compartment shrunk and therefore appeared brighter in the radiographs; and (b) these roots received D_2O from the main root axes (root transporting D_2O upwards during the day), either via diffusion or HR (convection). The root shrinkage was not the case as we did not detect any change of root shrinking–swelling overnight (Supplemental Figure S3). Therefore, we conclude that increasing transparency of the laterals of the sample shown in Figure 1 was caused by an increase of D_2O concentration. As laterals showed no growth and no detectable swelling, as observed in control experiments, a convective flow of water toward the lateral root tips means that water predominantly moved into the soil. On the contrary, nodal roots did grow. The convective fluxes toward the tip of nodal roots delivered water to the growing root tip. The efflux of water from the two nodal roots varied between the two roots. For the shorter one, the flux of water into the soil was similar to that from the lateral roots. For the longer roots, the flux of water into the soil was negligible. The differences in j_r between the two nodal roots might be explained by their different length and growth rate. The faster growth rate of the longer nodal root (3.4 cm per 15.5 h, compared with 1.2 cm per 15.5 h for the shorter nodal) is likely to have caused a stronger suction at the root tip (to drive water toward the tip) and consequently along all the root, decreasing the gradient in water potential between the root and the soil needed to drive the water efflux into the soil. Additionally, the root radial hydraulic conductivity typically decreases with increasing distance from the root tip (Meunier et al., 2018), which might have further reduced the water efflux from the long nodal root. These results show that HR varies between root types, and that the fraction of water that sustains root growth (dominant for nodal roots) and the one that flows into the soil (dominant for laterals) vary even more. The estimated fluxes are summarized in Figure 5.

The convective fluxes were estimated using inverse modeling. The model was needed to separate the effect of diffusion from that of convection. Therefore, the estimations are affected by the model assumptions. Relevant assumptions are constant diffusion coefficient during day and night, and uniform diffusion coefficient within the root tissue. These assumptions were instrumental to keep our model as simple as possible and to reduce the number of unknowns in the inverse problem. The assumption of uniform diffusion coefficient within the root tissue was tested by Zarebanadkouki et al. (2014), who showed that the model results were not sensitive to the different pathways across the root. An additional assumption was that roots did not swell and shrink during the experiments. Root swelling (shrinking) would cause an underestimation (overestimation) of D_2O concentration and, thus, of the HR. However, the test with H_2O showed no detectable changes in root volume and water content in our experiment.

It has to be noted that the reported measurements are specific of the tested setup, in which the small container size (40-cm depth), the use of sandy substrate, and the low number of replicates might limit the generalization of the estimated fluxes.

Despite these limits, we have shown how to quantify HR by combining neutron radiography, injection of D_2O, and a diffusion–convection model. For young maize, HR was highly variable along the root system and was root type specific. In conclusion, this method can be used for quantitative estimation of the spatial distribution of hydraulic lift in detailed laboratory experiments.

CONFLICT OF INTEREST

The authors declare no conflict of interest.

ACKNOWLEDGMENTS

Faisal Hayat was funded by the Ministry of Higher Education Commission, Pakistan under Contract no. 50015636. We thank Prof. Dr. Thomas Buecherl & the Heinz Maier-Leibnitz center team (The Technical University of Munich) for their precious technical support during the neutron radiography experiments.

REFERENCES

Ahmed, M. A., Zarebanadkouki, M., Kaestner, A., & Carminati, A. (2016). Measurements of water uptake of maize roots: The key function of lateral roots. *Plant and Soil*, *398*, 59–77. https://doi.org/10.1007/s11104-015-2639-6

Ahmed, M. A., Zarebanadkouki, M., Meunier, F., Javaux, M., Kaestner, A., & Carminati, A. (2018). Root type matters: Measurement of water uptake by seminal, crown, and lateral roots in maize. *Journal of Experimental Botany*, *69*, 1199–1206. https://doi.org/10.1093/jxb/erx439

Bauerle, T. L., Richards, J. H., Smart, D. R., & Eissenstat, D. M. (2008). Importance of internal hydraulic redistribution for prolonging the lifespan of roots in dry soil. *Plant, Cell & Environment*, *31*, 177–186. https://doi.org/10.1111/j.1365-3040.2007.01749.x

Brooks, J. R., Meinzer, F. C., Coulombe, R., & Gregg, J. (2002). Hydraulic redistribution of soil water during summer drought in two contrasting Pacific Northwest coniferous forests. *Tree Physiology*, *22*, 1107–1117. https://doi.org/10.1093/treephys/22.15-16.1107

Bücherl, T., & Söllradl, S. (2015). NECTAR: Radiography and tomography station using fission neutrons. *Journal of Large-Scale Research Facilities*, *1*, 8–10. https://doi.org/10.17815/jlsrf-1-45

Burgess, S. S. O., Adams, M. A., Turner, N. C., & Ong, C. K. (1998). The redistribution of soil water by tree root systems. *Oecologia*, *115*, 306–311. https://doi.org/10.1007/s004420050521

Caldwell, M. M., Dawson, T. E., & Richards, J. H. (1998). Hydraulic lift: Consequences of water efflux from the roots of plants. *Oecologia*, *113*, 151–161. https://doi.org/10.1007/s004420050363

Caldwell, M. M., & Richards, J. H. (1989). Hydraulic lift: Water efflux from upper roots improves effectiveness of water uptake by deep roots. *Oecologia*, *79*, 1–5. https://doi.org/10.1007/BF00378231

Carminati, A., Moradi, A. B., Vetterlein, D., Vontobel, P., Lehmann, E., Weller, U., … Oswald, S. E. (2010). Dynamics of soil water content in the rhizosphere. *Plant and Soil*, *332*, 163–176. https://doi.org/10.1007/s11104-010-0283-8

Carminati, A., & Zarebanadkouki, M. (2013). Comment on: "Neutron imaging reveals internal plant water dynamics." *Plant and Soil*, *369*, 25–27. https://doi.org/10.1007/s11104-013-1780-3

Hayat, F., Ahmed, M. A., Zarebanadkouki, M., Javaux, M., Cai, G., & Carminati, A. (2020). Transpiration reduction in maize (*Zea mays* L) in response to soil drying. *Frontiers in Plant Science*, *10*. https://doi.org/10.3389/fpls.2019.01695

Kasperl, S., & Vontobel, P. (2005). Application of an iterative artefact reduction method to neutron tomography. *Nuclear Instruments and Methods in Physics Research Section A: Accelerators, Spectrometers, Detectors and Associated Equipment*, *542*, 392–398. https://doi.org/10.1016/J.NIMA.2005.01.167

Meunier, F., Zarebanadkouki, M., Ahmed, M. A., Carminati, A., Couvreur, V., & Javaux, M. (2018). Hydraulic conductivity of soil-grown lupine and maize unbranched roots and maize root-shoot junctions. *Journal of Plant Physiology*, *227*, 31–44. https://doi.org/10.1016/j.jplph.2017.12.019

Millington, R. J., & Quirk, J. P. (1959). Permeability of porous media. *Nature*, *183*, 387–388. https://doi.org/10.1038/183387a0

Moradi, A. B., Carminati, A., Vetterlein, D., Vontobel, P., Lehmann, E., Weller, U., … Oswald, S. E. (2011). Three-dimensional visualization and quantification of water content in the rhizosphere. *New Phytologist*, *192*, 653–663. https://doi.org/10.1111/j.1469-8137.2011.03826.x

Mühlbauer, M. J., Bücherl, T., Kellermeier, M., Knapp, M., Makowska, M., Schulz, M., … Ehrenberg, H. (2018). Neutron imaging with fission and thermal neutrons at NECTAR at MLZ. *Physica B: Condensed Matter*, *551*, 359–363. https://doi.org/10.1016/j.physb.2017.11.088

Oswald, S. E., Menon, M., Carminati, A., Vontobel, P., Lehmann, E., & Schulin, R. (2008). Quantitative imaging of infiltration, root growth, and root water uptake via neutron radiography. *Vadose Zone Journal*, *7*, 1035–1047. https://doi.org/10.2136/vzj2007.0156

Richards, J. H., & Caldwell, M. M. (1987). Hydraulic lift: Substantial nocturnal water transport between soil layers by *Artemisia tridentata* roots. *Oecologia*, *73*, 486–489. https://doi.org/10.1007/BF00379405

Sharp, R. E., & Davies, W. J. (1985). Root growth and water uptake by maize plants in drying soil. *Journal of Experimental Botany*, *36*, 1441–1456. https://doi.org/10.1093/jxb/36.9.1441

Smart, D. R., Carlisle, E., Goebel, M., & Núñez, B. A. (2005). Transverse hydraulic redistribution by a grapevine. *Plant, Cell & Environment*, *28*, 157–166. https://doi.org/10.1111/j.1365-3040.2004.01254.x

Snyder, K. A., James, J. J., Richards, J. H., & Donovan, L. A. (2008). Does hydraulic lift or nighttime transpiration facilitate nitrogen acquisition? *Plant and Soil*, *306*, 159–166. https://doi.org/10.1007/s11104-008-9567-7

Tumlinson, L. G., Liu, H., Silk, W. K., & Hopmans, J. (2008). Thermal neutron computed tomography of soil water and plant roots. *Soil Science Society of America Journal*, *72*, 1234–1242. https://doi.org/10.2136/sssaj2007.0302

Wang, X., Tang, C., Guppy, C. N., & Sale, P. W. G. (2009). The role of hydraulic lift and subsoil P placement in P uptake of cotton (*Gossypium hirsutum* L.). *Plant and Soil*, *325*, 263–275. https://doi.org/10.1007/s11104-009-9977-1

Warren, J. M., Bilheux, H., Cheng, C. L., & Perfect, E. (2013). Reply to: Comment on "neutron imaging reveals internal plant water dynamics." *Plant and Soil*, *371*, 15–17. https://doi.org/10.1007/s11104-013-1858-y

Warren, J. M., Bilheux, H., Kang, M., Voisin, S., Cheng, C., Horita, J., & Perfect, E. (2013). Neutron imaging reveals internal plant water dynamics. *Plant and Soil*, *366*, 683–693. https://doi.org/10.2307/42952412

Zarebanadkouki, M., Kim, Y. X., & Carminati, A. (2013). Where do roots take up water? Neutron radiography of water flow into the roots of transpiring plants growing in soil. *New Phytologist*, *199*, 1034–1044. https://doi.org/10.1111/nph.12330

Zarebanadkouki, M., Kim, Y. X., Moradi, A. B., Vogel, H. J., Kaestner, A., & Carminati, A. (2012). Quantification and modeling of local root water uptake using neutron radiography and deuterated water. *Vadose Zone Journal*, *11*(3). https://doi.org/10.2136/vzj2011.0196

Zarebanadkouki, M., Kroener, E., Kaestner, A., & Carminati, A. (2014). Visualization of root water uptake: Quantification of deuterated water transport in roots using neutron radiography and numerical modeling. *Plant Physiology*, *166*, 487–499. https://doi.org/10.1104/pp.114.243212

Zegada-Lizarazu, W., & Iijima, M. (2004). Hydrogen stable isotope analysis of water acquisition ability of deep roots and hydraulic lift in sixteen food crop species. *Plant Production Science*, *7*, 427–434. https://doi.org/10.1626/pps.7.427

SUPPORTING INFORMATION

Additional supporting information may be found online in the Supporting Information section at the end of the article.

How to cite this article: Hayat F, Zarebanadkouki M, Ahmed MA, Buecherl T, Carminati A. Quantification of hydraulic redistribution in maize roots using neutron radiography. *Vadose Zone J.* 2020;19:e20084. https://doi.org/10.1002/vzj2.20084